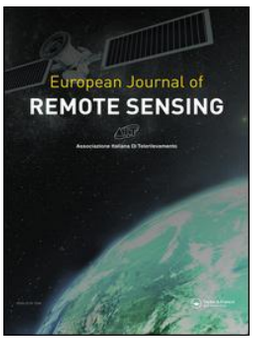

European Journal of Remote Sensing

ISSN: (Print) 2279-7254 (Online) Journal homepage: http://www.tandfonline.com/loi/tejr20

Quantitative mapping of clay minerals using airborne imaging spectroscopy: new data on Mugello (Italy) from SIM-GA prototypal sensor

Francesca Garfagnoli, Andrea Ciampalini, Sandro Moretti, Leandro Chiarantini & Silvia Vettori

To cite this article: Francesca Garfagnoli, Andrea Ciampalini, Sandro Moretti, Leandro Chiarantini & Silvia Vettori (2013) Quantitative mapping of clay minerals using airborne imaging spectroscopy: new data on Mugello (Italy) from SIM-GA prototypal sensor, European Journal of Remote Sensing, 46:1, 1-17, DOI: 10.5721/EuJRS20134601

To link to this article: https://doi.org/10.5721/EuJRS20134601

Published online: 17 Feb 2017.

Published by AIT
the Italian Society of Remote Sensing

Quantitative mapping of clay minerals using airborne imaging spectroscopy: new data on Mugello (Italy) from SIM-GA prototypal sensor

Francesca Garfagnoli[1*], Andrea Ciampalini[1], Sandro Moretti[1], Leandro Chiarantini[2] and Silvia Vettori[3]

[1]Department of Earth Sciences, University of Firenze, Via G. La Pira 4, 50121 Firenze, Italy
[2]Selex Galileo S.p.A., Via Albert Einstein 35, 50013 Campi Bisenzio (FI), Italy
[3]Department of Restoration and Conservation of Architectural Heritage, University of Firenze, Via Pier Antonio Micheli 8, 50121 Firenze, Italy
*Corresponding author, e-mail address: francesca.garfagnoli@unifi.it

Abstract
The possibility of using high spectral and spatial resolution remote sensing technologies is becoming increasingly important in the monitoring of soil degradation processes. A high spatial resolution hyperspectral dataset was acquired with the airborne Hyper SIM-GA sensor from Selex Galileo, simultaneously with ground soil spectral signatures and samples collection. A complete mapping procedure was developed using the 2000-2450 nm spectral region, demonstrating that the 2200 absorption band allows the obtainment of reliable maps of the clay content. The correlation achieved between the observed and the predicted values is encouraging for the extensive application of this technique in soil conservation planning and protection actions.
Keywords: Hyperspectral, soil mapping, clay minerals, SIM-GA.

Introduction
Since 2002, soils have been considered by the European Commission to be a non-renewable natural resource threatened by natural hazards and human activities (COM179/2002; http://www.dps.tesoro.it/documentazione/docs/all/normativa_europea/A_Azioni%20Strutturali/A1_Regolamenti%20del%20Consiglio/Reg_179_2002.pdf), such as erosion, organic matter decline, contamination, salinisation, floods and landslides. Soils under threat have worse performances in their environmental, economic, social and cultural functions.
High resolution and accurate maps of soil properties are needed to assess and avert soil degradation, to protect soil functions and to evolve to the sustainable exploitation and management of soils in agricultural practice. The goal of the EU FP7 project DIGISOIL [http://digisoil.brgm.fr/default.aspx; http://eusoils.jrc.ec.europa.eu/projects/Digisoil] is to enhance digital soil mapping by using and validating cutting edge geophysical sensing

European Journal of Remote Sensing - 2013, 46: 1-17
doi: 10.5721/EuJRS20134601

technologies. In particular, the DIGISOIL project aims at integrating and improving proximal and airborne technologies for the assessment of soil properties and soil degradation indicators for the production of digital high-resolution maps. The ultimate purpose is achieved through the validation of geophysical technologies and related pedo-geophysical inversion techniques and, because of the integration of the derived soil properties, for mapping soil functions and threats.

Governments around the world are undertaking programs to produce soil databases and maps to use in landscape planning and agricultural management (http://eusoils.jrc.ec.europa.eu/esdb_archive/raster_archive/sgdbe_display_attributes.html; http://soils.usda.gov/; http://webarchive.iiasa.ac.at/Research/LUC/External-World-soil-database/HTML/). In this framework, soil mapping is an essential tool in landscape management and planning because of the increasing demand for high-quality land-resource evaluation. In Italy for instance, because of the mainly hilly morphology, many of the agricultural soils are threatened and degraded by relief modelling processes, such as erosion and landslides, whose effects are added to the anthropic activities. Detailed catchment scale or farm scale maps of soil variability that provide fine spatial resolution are required to evaluate soil threats.

Traditional techniques for soil mapping are usually prohibitively expensive and time consuming [Sumfleth and Duttmann, 2007], involving the interpretation of aerial photography combined with the knowledge of correlations between soils and terrain properties. The application of these techniques is often difficult because they are mostly qualitative. The soil mapping units used in these traditional maps are considered homogeneous in terms of observed soil characteristics, but they represent more complex soils. The comprehension of both soil erosion processes and detailed soil characteristics' distribution is very important for the economic productivity of the agricultural system, as they affect geomorphic processes and the fertility of the surface. For this reason, researchers are progressively turning to remote sensing and, in particular, to reflectance spectroscopy, for the rapid and cost-effective development of maps of geological and mineralogical features [Bower and Rowan, 1996; Clark, 1999; Viscarra Rossel et al., 2006a,b; Ciampalini et al., 2012]. Moreover, the new airborne or satellite-based imaging spectrometers, working in the visible (VIS: 400-700 nm), near-infrared (NIR: 700-1300 nm) and short-wave infrared (SWIR: 1300-2500 nm) ranges, offer the possibility to directly realise high-resolution raster-based maps of soil properties. The chemical and mineralogical compositions of a soil are particularly variable because they depend both on the characteristics of the weathered parent rocks and minerals and on the different environmental conditions. In hyperspectral imaging, or imaging spectroscopy, each pixel in the image thus contains a continuous spectrum (in radiance or reflectance) and can be used to characterise the objects in the scene with great precision and detail. Hence, hyperspectral sensors provide a vastly improved ability to classify the objects in the scene based on their spectral properties [Goetz et al., 1985; Vane and Goetz, 1988; Green et al., 1998; Plaza et al., 2009].

The objective of this paper is to develop a new complete procedure for mapping soil features beginning with high-spectral and spatial resolution imagery. In particular, the possibility of predicting and mapping selected soil surface properties by testing the new prototypal sensor SIM-GA from Selex Galileo, working in the 350-2500 nm wavelength range, is investigated, focusing specifically on those properties that are indicators of soils'

vulnerability and agricultural capability. Among them, the clay content is considered to be useful to quantify the soil's vulnerability to erosion [Le Bissonnais, 1996; Madeira Netto et al., 2006; Lagacherie et al., 2008]. This study was performed in the DIGISOIL test site of Mugello, north of Firenze (Italy), where agricultural soils are widely threatened by surface processes, such as erosion and landslides. Based on this area, a cost-effective and time-saving complete mapping procedure, which allows the obtainment of fine-resolution catchment scale maps of soil features, is proposed and described below.

Materials and Methods

Study area

The test area is located approximately 30 km north of Firenze and it extends for approximately 20 km^2 to the north of the Sieve stream, a left tributary of the Arno river, centred in the Figliano airport and located between the villages of Borgo San Lorenzo, Luco di Mugello and Scarperia (Fig. 1).

The out-cropping geological terrains in these zones are Pliocene-Upper Pleistocene fluvio-lacustrine deposits that form low-dipping lenticular beds (CARG Project, Sheet 264 - Borgo S. Lorenzo). The landscape is typical of Tuscan intermontane basins, with gentle hills with low-altitude moderately dipping or level surfaces of alluvial origin, as well as fairly inclined to highly inclined slopes. The hills are subjected to both intense massive and superficial erosive processes. The climate is temperate to hot, with cold winters and mildly warm to hot summers and medium to intense rainfalls that are concentrated in the autumnal months. Average annual temperatures are around 11-12°C in the month of January, with average values of about 6°C, while during the summer season, between July and August, average temperatures reach the value of 22-23°C. The cumulative average annual precipitation is around 1100 mm. Agriculturally suitable terrains are assigned mainly to annual crops and marginally to olive groves, vineyards and orchards. The grain size of the selected parcels generally spans from silty sand to silty clay [Benvenuti, 2003].

From a pedologic point of view, the soils on the eastern side of the study area (Borgo San Lorenzo and Figliano side: see Fig. 1) are characterised by a muddy texture and a coarse prismatic framework. They are wide, not very deep and barely drained. The regolith is represented by lacustrine mud, with intercalations of cohesive reddish silty layers. Vermiculite and montmorillonite have been detected within the lacustrine mud [Benvenuti, 2003]. These soils show widespread cracks, up to 4 cm deep, developed during the dry season. The western side of the study area (Scarperia side: Fig. 1) is characterised by a similar landscape, but the topsoils of the hills show an intense accumulation of mud and oxides in the B horizon. Gley processes in the B and C horizons are favoured by the stagnation of water, suggesting poor drainage. The soils are deep, and the grain size is dominated by fine mud. The erosive processes are not homogeneous. The pH varies from acid to neutral, and the carbonates are almost absent. The parent material is represented by Medium to Upper Quaternary fluvial sands and gravels and subordinately by lacustrine mud. The bottoms of the hills are characterised by thin muddy soils, which are moderately alkaline, rich in carbonates and well drained. In this case, the parent material is represented by lacustrine mud with the intercalation of very fine sands [Benvenuti, 2003].

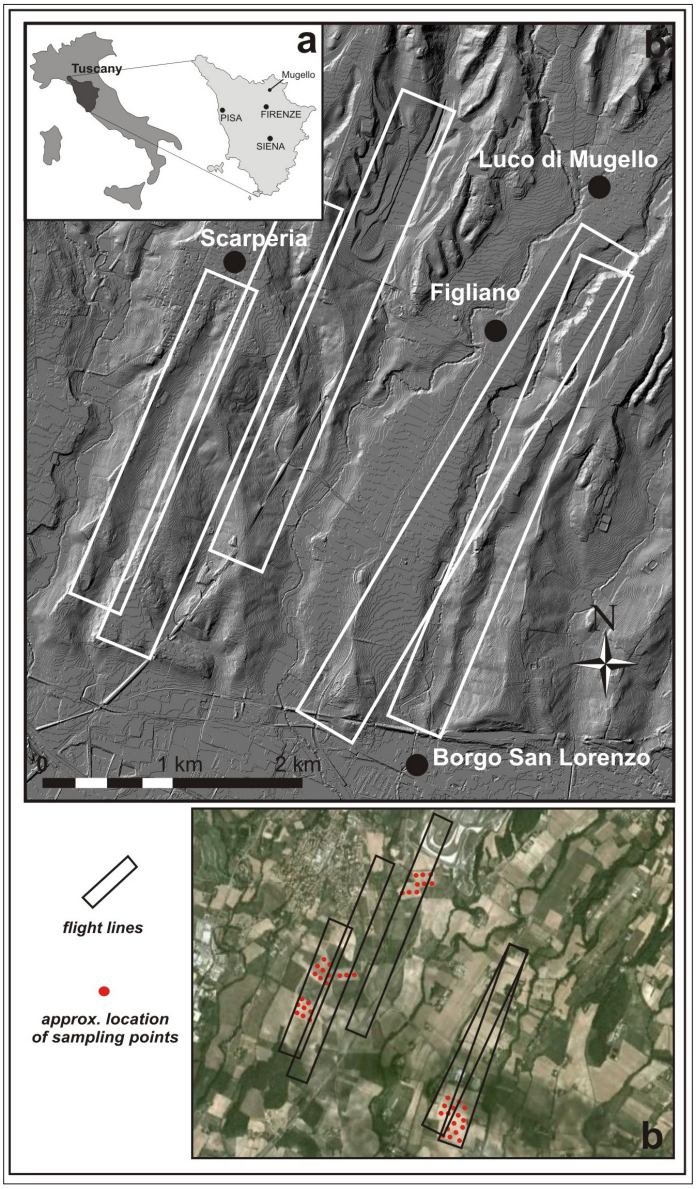

Figure 1 - Location of study area and overview of flight lines and sampling locations.

Hyperspectral imagery acquisition and soil sample collection

In the context of the DIGISOIL project, the prototypal airborne hyperspectral imager SIM-GA from Selex Galileo was tested and improved.

The Multisensor Hyperspectral System, produced by Selex Galileo (Hyper SIM-GA), is an experimental modular pushbroom avionic hyperspectral imager, composed of two electro-optical heads in the VNIR and SWIR spectral range (from 400 nm to 2450 nm) and a digital

acquisition system, which acquires nadir images with a continuous spectral sampling of more than 700 channels. In comparison, for instance, the most used airborne imaging spectrometers, such as AVIRIS from NASA/Jet Propulsion Laboratory (http://aviris.jpl.nasa.gov/ and HYMAP from Integrated Spectronics (http://www.intspec.com/products/HyMap/overview/) have 224 [Porter and Enmark, 1987; Green et al., 1998] and 126 [Cocks et al., 1998] bands, respectively.

The SIM-GA average sampling intervals are 1.2 nm (VNIR) and 5.8 nm (SWIR). The instantaneous field of view is 0.7 mrad in the VNIR and 1.3 mrad in the SWIR portions of the spectrum. Spectral pixels are 512 and 256 for VNIR and SWIR, respectively. With the SIM-GA modular approach, the two optical heads are physically separated but installed on a common support plate, and their fields of view result in a co-alignment to a common inertial/GPS unit; this allows the acquisition of data for geo-referentiation and ortho-rectification of the images, as well as a correction for stability changes during the flight. This concept permits a flexible application-driven configuration of the instrument and its installation both on a static scanning platform for ground-based applications and on airborne platforms, including ultralight aircrafts (ULM). Data are delivered to the acquisition system, which processes and stores them on removable hard-disks.

After two preliminary test flight campaigns (for installation of SIM-GA on board the University of Firenze ultralight aircraft, flight software updating and boresight geometric calibration of the sensor), the hyperspectral images were acquired in September 2009. This period was selected for the flight and ground data collection, according to the typical climate in Italy, to ensure a cloudless sky, high sun illumination conditions and a large availability of bare fields, depending on crop rotation in the study area. A pilot field survey allowed the establishment of a flight plan that included five flight paths approximately 350 m wide and 3-5 km long (Fig. 1). The approximate pixel resolution was 0.6 m (VNIR) and 1.2 m (SWIR), considering a height of flight of about 900 m. Contemporaneously, some of the parcels characterised by bare soils were sampled (more or less 1.5 kg of topsoil up to 3 cm in depth), following a regular grid according to the dimension of each field, for a total of about 40 samples. The positions of the samples were recorded with a differential GPS receiver (Leica 1200, 3-4 cm spatial accuracy).

Pre-processing and data elaboration techniques

The collected SIM-GA raw data include separate VNIR and SWIR raw DN data blocks in an ENVI format and navigation INS/GPS data. The SIM-GA row data were first transformed into at-sensor radiance values, applying sensor calibration coefficients and parameters from laboratory measurements to non-georeferenced VNIR/SWIR digital number values.

Radiometrically calibrated at-sensor radiance data were then corrected for the influence of atmosphere, solar illumination, sensor viewing geometry and terrain geometry information and inverted into geometrically and atmospherically corrected at-surface reflectance values that are useful for the retrieval of inherent surface reflectance properties. Surface reflectance is commonly considered as the basic product, which is a function of several geophysical parameters that have to be investigated and retrieved by means of inversion algorithms.

The geometric correction is accomplished before the atmospheric correction. Distortions may be caused by the geometric characteristics of the sensor itself, variation in the position and orientation of the sensor (pitch, yaw and roll) and relief displacements. Geocoded

products are retrieved for each flight line with a model-based procedure (direct georefencing), developed in the IDL language and PARGE (PARametric Geocoding, ReSe Applications Schäpfler and RSL, University of Zurich) software, which exploits the inertial navigation system (INS) and differentially corrected GPS data (latitude, longitude, height) recorded in the aircraft, to ortho-rectify an image over a 1-m cell digital elevation model (DEM), especially produced for this aim, with an aero-photogrammetric and topographic survey. The PARGE outputs for each HYPER image include *.igm files (Lat/Long Geographic LUT for ENVI) and *.sca files (scan zenith/azimuth angles and the altitude for ENVI).
The atmospheric correction was achieved using the physically based model FLAASH (Fast Line-of-sight Atmospheric Analysis of Spectral Hypercubes), which considers only the medium value of altitude in the image and adopts MODTRAN (MODerate resolution TRANsmitance, from the Air Force Research Lab, Space Vehicles Directorate, USA) codes as a model to simulate the calculation of radiative transfer [Anderson et al., 1995]. Measured or modelled input variables, such as atmospheric conditions (e.g., optical depth) and geometry information (flight altitude, illumination and viewing angles) are required as input parameters, allowing the atmospheric configuration to be modelled.
When all compensation parameters are applied to the hyperspectral data, ortho-rectified, geo-referenced and co-registered VNIR to SWIR images are available for atmospheric correction over the full 400-2500 nm spectral range, as well as for the use/application in GIS environment and 3D view.
Once the reflectance image is obtained, it typically undergoes spectral classification: each pixel of the image is classified based on spectral resemblance, depending on the occurrence of a certain material and possibly on its relative abundance. Hereafter, instead, a new procedure for the inversion of images into abundance maps using ENVI software (ITT VIS, Boulder, CO) is proposed.

Laboratory soil analysis

The 40 samples collected during the field campaign underwent traditional laboratory analyses to determine the clay minerals' content. After drying for a week, quartering and crushing to fine-earth grain size, approximately 50 g of material was passed through a 2-mm sieve and then pulverised to obtain a powder grain size, suitable for an XRD analysis. The dataset was split into two subsets: one was used to define the experimental inversion procedure (training set), and the second was interpolated to obtain the validation map of the observed clay values (validation set).
The mineral composition, including clay minerals, was determined by means of XRD with a Rietveld refinement [Lutterotti et al., 1997, 2007]. This procedure has specifically been created for clay minerals, which generally show preferential orientation, layer intermixing, turbostatic disorder and variability in interlayer water and cations. The subsequent step was the qualitative analysis, which allows recognition of the phases through a search-match of the peaks. Then, images were processed with the Rietveld code MAUD [Lutterotti et al., 1997, 2007] using the single layer theory [Ufer et al., 2004, 2008], to take into account the turbostatic disorder.
Laboratory spectral signatures were collected using an ASD FieldSpec Pro spectrometer, which measures reflectance in 3-10 nm bandwidths over the 350-2500 nm range. A dedicated nadir viewing set-up, including two halogen tungsten lamps (24 V; 70 W) connected with

a stabilised power supply device (TTi EX354D; Dual Output; 35V; 4A; 280W) was used to ensure minimum shadowing perturbation and to guarantee the control of the irradiance conditions. Lamps are located laterally with respect to the sample, at a distance of 60 cm and inclined at 45°. The optic fibre is in the nadir position at a height of 5-10 cm above the sample, resulting in a table-projected field of view diameter of 2-4.5 cm. All measurements were performed on both raw samples and on the powders. In the latter case, special care was used in levelling the powder to a uniform thickness. For each sample surface, four averages of 100 reflectance measurements were acquired in different positions, in order to reduce noise, while reference measurements on the Spectralon panel were averaged on the 100 spectra and repeated systematically every three samples. The four mean spectra acquired in the different positions were averaged using the ASD ViewSpec Pro, and possible "steps" in the spectrum were eliminated using the "splice correction" function of this software. Normalisation, exclusion of noisy tales and the continuum removal (see next paragraph) from spectra were obtained using a dedicated script, developed in Matlab (The Matworks, Natick, MA) language, which transforms the entire spectral library into the ASCII format simultaneously.

Continuum removal analysis

Among the techniques used to relate soil spectral features to soil parameters, two methods are usually preferred: partial least square regression (PLSR) and continuum removal (CR). Many previous studies have examined the capability of VNIR/SWIR spectroscopy to quantify, predict and map soil properties through CR and PLSR, beginning with laboratory [Walvoort and McBratney, 2001; Cozzolino and Moron, 2003; Madeira Netto et al., 2006; Lagacherie et al., 2008] and airborne or satellite hyperspectral data [Crouvi et al., 2006; Selige et al., 2006; Poulet et al., 2007; Galvão et al., 2008; Lagacherie et al., 2008]. These studies have proved that airborne or satellite hyperspectral data can be used in mapping soil properties, although these latter are generally affected by limitations due to atmospheric effects, the signal to noise ratio of the instrument and the occurrence of spectral mixtures in soil pixel surfaces.

Continuum removal, with respect to other statistical approaches, provides more casual correlations between the spectral features and the related amount of absorbing material [Lagacherie et al., 2008]. This approach is based on the fact that the depth of an absorption feature, at a certain wavelength, is strongly related to the abundance of the absorbing material. Continuum removal normalises the reflectance spectra, with the aim of allowing a direct comparison among the absorption features from a common baseline, minimising the effects of different scales or observation conditions and presupposing that no other mineral has strong absorptions around that particular wavelength [Clark and Roush, 1984]. In particular, reflectance curves typically show a convex shape, with wide and shallow absorption features, which make it difficult to identify and quantify such features, in terms of position, depth, width, area and asymmetry [Leone, 2000]. Moreover, these parameters are strongly influenced by the peak position in the background. All of these difficulties can be avoided by normalisation with the "convex-hull" technique [Green and Craig, 1985], which aims at eliminating the convex shape of the acquired signal and enables the relation of different samples over the same reference [Kokaly, 2001]. In this paper, normalisation was achieved through the "convex-hull quotients" technique [Van der Meer, 1995], according to which:

$$R'(\lambda) = Rb(\lambda)/Rc(\lambda), \quad [1]$$

where Rb is the reflectance of a certain peak at the wavelength λ, and Rc is the reflectance of the continuum at the same wavelength. Once the spectra are normalised, the absorption peak depth can be calculated, following Clark and Roush [1984], as:

$$Db(\lambda) = 1 - R'(\lambda). \quad [2]$$

Clay content and mineralogy influence the SWIR portion of the spectrum (1300-2500 nm), with the 2200 absorption feature being characteristic of clays [Ben-Dor, 2002]. Soil texture and mineralogy have been related to the depth of the clay absorption peaks [Ben-Dor and Banin, 1995] or to the statistical analysis of the form of the whole spectra [Brown et al., 2006; Viscarra Rossel et al., 2006b].
After CR, the absorption peak depth at a specific wavelength is calculated and related to the atomic group responsible for the spectral feature, such as, for instance, the values at 2206 and 2341 nm for clay and calcium carbonate, respectively [Chabrillat et al., 2002]. Considering a specific absorption peak, the continuum is represented by a straight line that connects the two local reflectance maxima corresponding to the shoulders (λ_{min} and λ_{max}) of the peak (λ_{peak}). The absorption peak depth (APD_{λ}) is then a function of the reflectance $R(\lambda)$ at the wavelength λ, and its value cannot exceed 1. For total clays, absorption peaks are expected to be approximately 2206-2208 nm, due to the combination of OH and OH-Al bending [Chambrillat et al., 2002], or 2200 nm, corresponding to the absorption of OH in the clay lattice [Ben-Dor et al., 2009; Viscarra Rossel et al., 2006b]. Moreover, absorption features at approximately 1400 and 1900 nm are generally present and caused by the bending and stretching in the O-H bonds of free water. The visual observation of collected ASD spectra allowed precise positioning of clay absorption features, which were slightly modified with respect to the literature values into 1414, 1914 (water absorption features) and 2210 nm.
Then, linear regression was used to relate the clay content to the corresponding APD_{λ} values, according to the following expression:

$$Clay = \alpha_{Clay}(1 - APD_{2206}). \quad [3]$$

Results and discussion

Laboratory Soil Analysis

The results of the mineralogical analysis are shown in Table 1. The amount of clay in the samples ranges from 30% to more than 65% and is 50% on average. Montmorillonite and illite prevail, with minor amounts of kaolinite (Tab. 1).
The overall form of the ASD spectra are quite similar among the studied soil samples, except for differences in albedo and a few variations in the APD values for several spectral features. The prevalence of illite and montmorillonite in the study area is confirmed by the occurrence of a single symmetrical absorption feature at 2210 nm, which is diagnostic for these minerals (Fig. 2).

Table 1 - Statistics of clay minerals: laboratory results from mineralogical analysis (% weight percentage).

	Montm.	Illite	Kaolinite	Total
No. of samples	40	40	40	40
Mean	19.85	28.15	2.30	50.99
Median	21.62	27.65	3.07	51.02
Std. Deviation	10.04	4.15	1.47	9.04
Minimum	0	21.33	0.003	31.40
Maximum	35.51	36.94	6.17	66.63

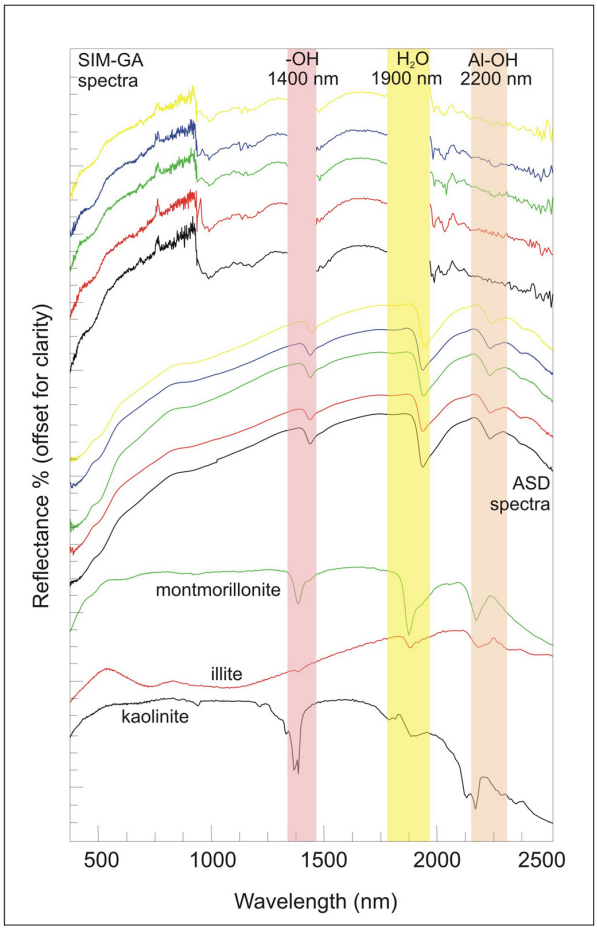

Figure 2 - VNIR and SWIR spectral profile comparing SIM-GA and ASD spectra and showing the main absorption features. Kaolinite, illite and montmorillonite spectra from USGS spectral library are also showed. Bands in the 1400 nm and 1900 nm atmospheric absorption windows have been omitted from SIM-GA profiles.

A clear relationship was observed between the clay content and APD1414 (R^2=0.70) and APD_{1914} (R^2=0.73), while the determination coefficient (R^2) between the clay content and APD_{2210} is 0.58 (Fig. 3).
This implies that the use of APD_{1414} or APD_{1914} in the mapping procedure might possibly improve the accuracy of the clay content prediction, but, unfortunately, in the case of airborne or satellite sensors, both of these peaks fall into the atmospheric absorption bands and cannot be used.
The strength of all of these relationships decreases significantly when the same procedure is applied to the SIM-GA data, as also observed by previous authors for other airborne sensors [Gomez et al., 2008; Lagacherie et al., 2008].

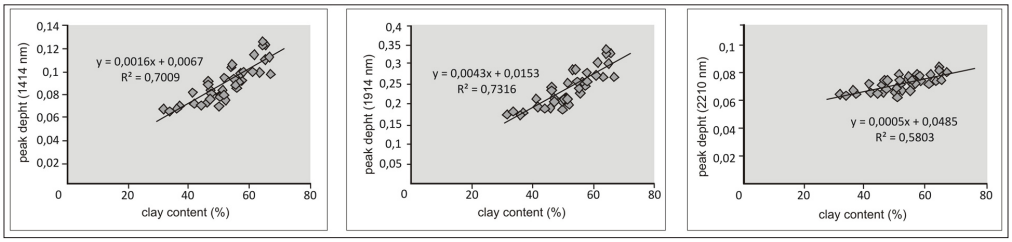

Figure 3 - Correlation between clay content and absorption peak depth at 1414 nm, 1914 nm and 2210 nm for ASD spectral data (vertical scale adapted).

Mapping of soil properties

A portion of the study area was used to test the correlation between the airborne hyperspectral data and the clay content values obtained through traditional laboratory analyses. The elaboration of clay content maps from the SIM-GA hyperspectral images was organised in the following steps:

1) normalisation of the spectra for each pixel of the SIM-GA image using the "continuum removal" function of the ENVI software;
2) based on the field training set, elaboration of the absorption peak depth map at 2210 through a dedicated IDL routine;
3) extraction of the absorption peak values corresponding to the actual location of each sampling point, after averaging within a 3×3 pixel square;
4) retrieval of the correlation between the values obtained at point 3), and the related laboratory ASD absorption peak depths at 2210, acquired from field samples;
5) inversion of the map elaborated at point 2) into a map of ASD absorption peak values, using the regression line obtained at point 4), corresponding to:

$$y = 8.1088x - 0.3683; \quad [4]$$

6) calculation of the regression between the values extrapolated from the map obtained at point 5), for each sampling point (averaged within a 3×3 pixel square) and the corresponding clay content value, obtained from samples;

7) inversion of the ASD absorption peak map into a predicted clay content map, using the regression lines calculated at point 6) for every single clay mineral and for total clay content (Tab. 2).

Table 2 - Regression lines used for each clay mineral.

Target mineral	Correlation line
Montmorillonite	y= -143.26x+36.269
Illite	y= 55.934x+22.838
Kaolinite	y= 18.281x+1.0012
Total Clay	y= -69.047x+60.108

The maps resulting from this procedure for each of the analysed clay minerals and for the total amount of clays are shown in Figure 4 in which brown corresponds to the higher percentages and blue corresponds to the lower percentages. A mask was applied to the neighbouring grassland. The maps of illite and of montmorillonite (Figs. 4a, b) show a similar trend, both having a normal correlation between the concentration determined with XRD and the absorption peak values. Lower values are clustered in the northern part of the parcel, which is topographically more elevated, while an increasing trend towards the south (i.e., parallel to the flow direction, towards the bottom) can be observed for both minerals. This tendency can be interpreted as a normal effect due to soil erosion by rain water and the consequent removal and concentration of finer material downhill. On the contrary, the map of kaolinite content (Fig. 4c) displays a completely inverted trend, with higher concentrations located to the northern and south-eastern parts of the field. As shown in Figure 4d, the distribution of the total clay content closely resembles that of illite and montmorillonite. A comparison among the maps shows that kaolinite scarcely affects the total clay areal distribution.

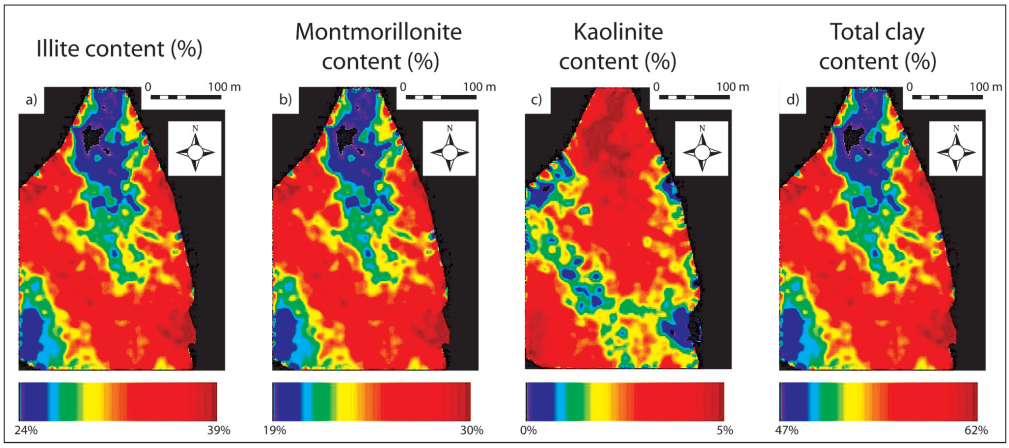

Figure 4 - Hyperspectral-derived clay map for illite (a), montorillonite (b), kaolinite (c) and total clay (d).

This may be related to two main causes: a) the very low concentrations of kaolinite with

respect to other clays, as has also been confirmed by mineralogical analysis on samples and/or b) the scarce correlation between XRD kaolinite contents and the related absorption peak depth values, possibly also due to the absorption feature being affected by noise and not particularly clearly resolved.
A reliability test for the described procedure can be performed using linear regression, which analyses the relationship between two variables, X and Y, finding the best straight calibration line through the data, with the goal of minimising the sum of the squares of the vertical distances of the points from the line. The calibration line was calculated between the hyperspectral-predicted clay values and their correspondent clay mineral content, observed in the sampling data set. The correlation between the two variables shows a determination coefficient of R^2=0.599 (Fig. 5); as a consequence, the model can explain approximately 60% of the actual variability of the clay content in the top level of soils for the studied area. In details, the predicted clay content underestimates the actual value (approx. 50%).

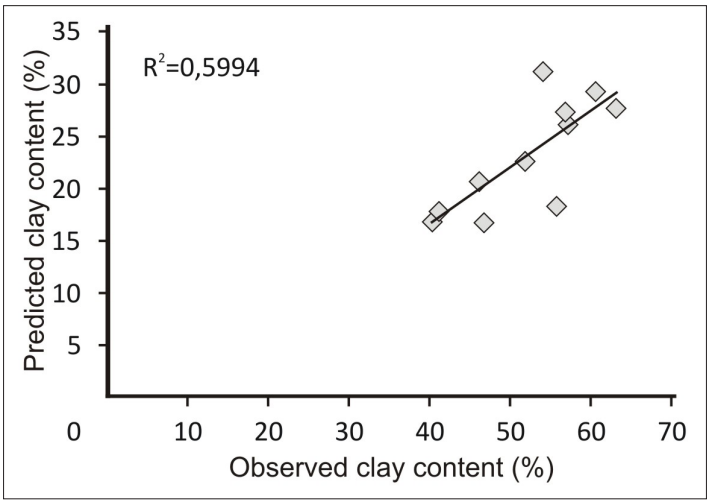

Figure 5 - Plot of the linear regression between clay content predicted using SIM-GA and from the validation sampling data set.

For validation, the predicted clay content map, deduced from hyperspectral data, was compared with the interpolated geographic distributions of the validation set clay content values (observed soil property), obtained from the field specimens, using the Inverse Distance Weighting algorithm (Fig. 6). These maps represent the spatial variability of the ground truth data. The value ranges show a general consistency between measured and predicted properties; the areal pattern, with a minimum located at the northern tip of the parcel, appears similar for illite, montmorillonite and total clay (Figs. 6a, b, d), except for local variations, confirming an enrichment in clays towards the valley bottom due to erosion. On the contrary, there is an evident mismatch between the predicted and the observed (Fig. 6c) trends of kaolinite. This unsatisfactory result can be related to the low concentrations of kaolinite in the sampled soils, which implies a reduced correlation between the XRD kaolinite contents and the related absorption peak depth values.

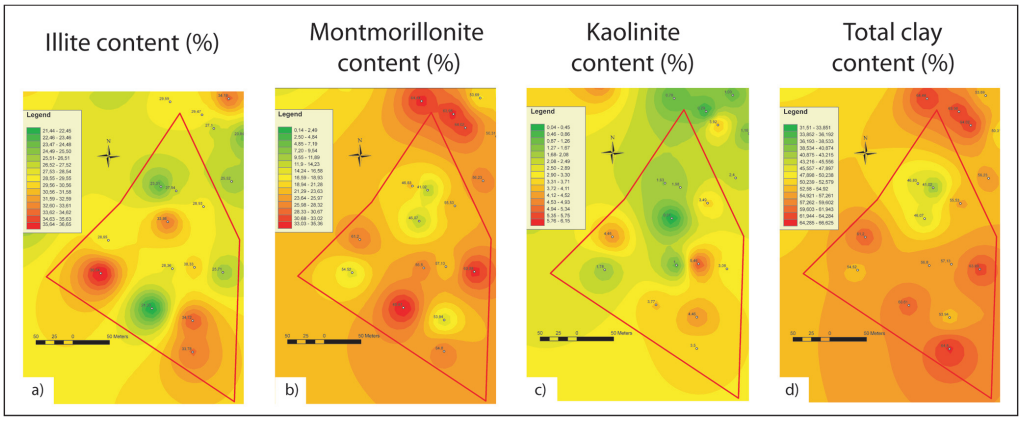

Figure 6 - Maps obtained from IDW interpolation of laboratory values, for illite (a), montorillonite (b), kaolinite (c) and total clay (d).

Conclusions

As demonstrated by Lagacherie et al. [2008], laboratory-calibrated relations can be applied to map soil surface properties from hyperspectral images. In this study, hyperspectral imagery in the visible/near infrared spectral ranges from a SIM-GA prototypal sensor, laboratory reflectance measurements of dried sifted samples, as well as mineralogical determinations of field samples are employed to map one of the most important soil properties, such as the content of clay mineral. Using the continuum removal approach, we demonstrate that the clay content in soils can be estimated from the reflectance data and that, in all cases in which the 1400 nm and the 1900 nm absorption features cannot be used (according to the sensor type and/or acquisition conditions), the absorption band located at approximately 2210 can be exploited to obtain reliable predictions. Moreover, a complete procedure for the inversion of images into clay maps is established and described.

Because imaging spectroscopy offers a rapid and cost-effective method for the prediction of soil properties with respect to traditional soil surveys and analysis, it could be profitably used to improve the spatial resolution in soil inventories and soil mapping projects. However, maps are defined relative to test sites; therefore, their spatial validity must be further investigated to evaluate the influence of different geomorphological, pedological and geological contexts. Moreover, the quality of the relationships between the soil's properties and spectral features decreases significantly from the laboratory-controlled reflectance measurements to the SIM-GA data, demonstrating that the performance of this technique is strongly dependent on the level of acquisition (laboratory or airborne) and possibly on the sensor as well. Thus, it could profit from an improvement in the quality of the collected hyperspectral images and from new, more accurate, atmospheric and radiometric correction algorithms.

The comparison between the hyperspectral-derived maps of clay and the correspondent IDW interpolations of the measured clay content values demonstrates that our results are encouraging and reliable, at least for illite, montmorillonite and total clay, whereas they should be considered with caution in the case of kaolinite. The inconsistency of the relation between the kaolinite observed and predicted data could be due to local factors and related to the very low concentration of this mineral. Kaolinite-rich soils should be investigated

more in detail to further evaluate the general effectiveness of the method described in this paper. Any future advance in this research should speculate on the possibility of applying the PLSR approach to the same datasets, especially for the analysis of scarcely significant absorption features, in order to include more spectral elements, which can be either directly or indirectly related to the studied property in the predictive model.
Nevertheless, the comparison of both the observed/predicted maps and the R^2 values obtained in this work with those elaborated with the PLSR approach and reported by Summers et al. [2011], indicates that the CR is an alternative and valid method in clay content mapping. Both studies demonstrate how raster maps of predicted soil properties can be simply and rapidly created and show good agreement with the measured values areal distribution.
Moreover, with respect to previous analogous studies [e.g. Chabrillat et al., 2002; Galvão et al., 2008; Gomez et al., 2008] this approach, favoured for the high number of bands (approximately 700) provided by the Hyper SIM-GA, offers a rapid and reliable potential for the quantification and mapping of the soil's parameters.
This method, tested for clay minerals, could be extended to a larger number of soil properties (calcium carbonates, iron oxides, etc.), which can be directly related to the reflectance spectra [Viscarra Rossel et al., 2006b] and thus widely used in the future for the rapid evaluation and digital mapping of other erosion-related soil features.

Acknowledgements

This research was supported by the DIGISOIL project. The DIGISOIL project is financed by the European Commission under the 7th Framework Programme for Research and Technological Development, Area "Environment", Activity 6.3 "Environmental Technologies". This paper reflects the author's views. The European Commission is not liable for any use that may be made of the information contained herein. The authors are indebted to Prof. E. Ben-Dor for his critical reading of the manuscript and constructive advices. We also acknowledge Dr. Gaia Righini and the anonymous reviewer for substantially improving the quality of the paper.

References

Anderson G.P., Kneizys F.X., Chetwynd J.H., Wang J., Hoke M.L., Rothman L.S., Kimball L.M., McClatchey R.A., Shettle E.P., Clough S.A., Gallery W.O., Abreu L.W., Selby J.E.A. (1995) - *FASCODE/MODTRAN/LOWTRAN: Past/Present/Future*. In: 18th Annual Review Conference on Atmospheric Transmission Models, Hanscom Air Force Base, MA.

Ben-Dor E. (2002) - *Quantitative remote sensing of soil properties*. Advances in Agronomy, 38: 1-44.

Ben-Dor E., Banin A. (1995) - *Near-infrared analysis (NIRA) as a method to simultaneously evaluate spectral featureless constituents in soils*. Soil Science, 159: 259-270. doi: http://dx.doi.org/10.1097/00010694-199504000-00005.

Ben-Dor E., Chabrillat S., Demattê J.A.M., Taylor G.R., Hill J., Whiting M.L., Sommer S. (2009) - *Using Imaging Spectroscopy to study soil properties*. Remote Sensing of Environment, 113: S38-S55. doi: http://dx.doi.org/10.1016/j.rse.2008.09.019.

Benvenuti M. (2003) - *Facies analysis and tectonic significance of lacustrine fan-deltaic successions in the Pliocene–Pleistocene Mugello Basin, Central Italy*. Sedimentary

Geology, 157 (3-4): 197-234. doi: http://dx.doi.org/10.1016/S0037-0738(02)00234-8.

Bower T.L., Rowan L.C. (1996) - *Remote mineralogic and lithological mapping of the Ice River alkaline complex, British Columbia, Canada, using AVIRIS data*. Photogrammetric Engineering and Remote Sensing, 62: 1143-1376.

Brown D.J., Shepherd K.D., Walsh M.G., Mays M.D., Reinsch T.G. (2006) - *Global soil characterization with VNIR diffuse reflectance spectroscopy*. Geoderma, 132: 273-290. doi: http://dx.doi.org/10.1016/j.geoderma.2005.04.025.

CARG Project, Sheet 264, Borgo S. Lorenzo, http://www.regione.toscana.it/regione/export/RT/sito-RT/Contenuti/sezioni/territorio/geologia/visualizza_asset.html_399098699.html.

Chabrillat S., Goetz A.F.H., Krosley L., Olsen H.W. (2002) - *Use of hyperspectral images in the identification and mapping of expansive clay soils and the role of spatial resolution*. Remote Sensing of Environment, 82: 431-445. doi: http://dx.doi.org/10.1016/S0034-4257(02)00060-3.

Ciampalini A., Garfagnoli F., Antonielli B., Moretti S., Righini G. (2012) - *Remote sensing techniques using Landsat ETM+ applied to the detection of iron ore deposits in Western Africa*. Arabian Journal of Geosciences. doi: http://dx.doi.org/10.1007/s12517-012-0725-0.

Clark R.N. (1999) - *Spectroscopy of rocks and minerals and principles of spectroscopy*. In: A. N. Rencz (Ed.), Remote Sensing for the Earth Sciences. John Wiley & Sons, Chichester, UK, pp. 3-58.

Clark R.N., Roush T.L. (1984) - *Reflectance spectroscopy: Quantitative analysis techniques for remote sensing applications*. Journal of Geophysical Research, 89: 6329-6340. doi: http://dx.doi.org/10.1029/JB089iB07p06329.

Commission of the European Communities (2002) - *Communication from the commission to the council, the european parliament, the economic and social committee and the committee of the regions. Towards a Thematic Strategy for Soil Protection*. Brussels, 16.4.2002 COM(2002) 179 final, pp 35.

Cocks T., Jenssen R., Stewart A., Wilson I., Shields T. (1998) - *The HyMapTM Airborne Hyperspectral Sensor: The System, Calibration and Performance*. In: Proceedings of the 1st EARSEL Workshop on Imaging Spectroscopy, 6-8 October 1998, Zurich, pp. 37-42.

Cozzolino D., Moron A. (2003) - *The potential of near-infrared reflectance spectroscopy to analyse soil chemical and physical characteristics*. Journal of Agricultural Sciences, 140: 65-71. doi: http://dx.doi.org/10.1017/S0021859602002836.

Crouvi O., Ben-dor E., Beyth M., Avigad D., Amit R. (2006) - *Quantitative mapping of arid alluvial fan surfaces using field spectrometer and hyperspectral remote sensing*. Remote Sensing of Environment, 104: 103-117. doi: http://dx.doi.org/10.1016/j.rse.2006.05.004.

Galvão L.S., Formaggio A.R., Couto E.G., Roberts D.A. (2008) - *Relationships between the mineralogical and chemical composition of tropical soils and topography from hyperspectral remote sensing data*. ISPRS Journal of Photogrammetry & Remote Sensing, 63 (2): 259-271. doi: http://dx.doi.org/10.1016/j.isprsjprs.2007.09.006.

Goetz A.F.H., Vane G., Solomon J.E., Rock B.N. (1985) - *Imaging spectrometry for earth remote sensing.* Science, 228: 1147-1153. doi: http://dx.doi.org/10.1126/science.228.4704.1147.

Gomez C., Lagacherie P., Coulouma G. (2008) - *Continuum removal versus PLSR method*

for clay and calcium carbonate content estimation from laboratory and airborne hyperspectral measurements. Geoderma, 148 (2): 141-148. doi: http://dx.doi.org/10.1016/j.geoderma.2008.09.016.

Green A.A., Craig M.D. (1985) - *Analysis of aircraft spectrometer data with logarithmic residuals*. In: Proceedings AIS workshop, April 8-10 1985, Jet Propulsion Laboratory, Pasadena, California, pp. 111-119.

Green R.O., Eastwood M.L., Sarture C.M., Chrien T.G., Aronsson M., Chippendale B.J., Faust J.A., Pauri B.E., Chovit C.J., Solis M., Olah M.R., Williams O. (1998) - *Imaging spectroscopy and the Airborne Visible/Infrared Imaging Spectrometer (AVIRIS)*. Remote Sensing of Environment, 65: 227-248. doi: http://dx.doi.org/10.1016/S0034-4257(98)00064-9.

Kokaly R.F. (2001) - *Investigating a physical basis for spectroscopic estimates of leaf nitrogen concentration.* Remote Sensing of Environment, 75 (2): 153-161. doi: http://dx.doi.org/10.1016/S0034-4257(00)00163-2.

Lagacherie P., Baret F., Feret J.B., Madeira Netto J., Robbez-Masson J.M. (2008) - *Estimation of soil clay and calcium carbonate using laboratory, field and airborne hyperspectral measurements*. Remote Sensing of Environment, 112: 825-835. doi: http://dx.doi.org/10.1016/j.rse.2007.06.014.

Le Bissonnais Y. (1996) - Aggregate stability and assessment of crustability and erodibility: I. Theory and methodology. European Journal of Soil Science, 47: 425-437. doi: http://dx.doi.org/10.1111/j.1365-2389.1996.tb01843.x.

Leone A. P. (2000) - *Spettrometria e valutazione della riflettanza spettrale dei suoli nel dominio ottico 400 – 2500 nm*. Rivista Italiana di Telerilevamento, 19: 3-28.

Lutterotti L., Bortolotti M., Ischia G., Lonardelli I., Wenk H.R. (2007) - Rietveld texture analysis from diffraction images. Zeitschrift für Kristallographie Supplements, 26: 125-130. doi: http://dx.doi.org/10.1524/zksu.2007.2007.suppl_26.125.

Lutterotti L., Matthies S., Wenk H.R., Schults A.J., Richardson J.W. (1997) - *Combined texture and structure analysis of deformed limestone from time-of-flight neutron diffraction spectra*. Journal of Applied Physics, 81: 594-600. doi: http://dx.doi.org/10.1063/1.364220.

Madeira Netto J.S.R., Robbez-Masson J.M., Martins E. (2006) - *Visible-NIR hyperspectral imagery for discriminating soil types in the La Peyne watershed (France)*. In Lagacherie P., Mc Bratney A.B. and Voltz M. (Eds.), Digital Soil Mapping: an Introductory Perspective, Elsevier Montpellier. doi: http://dx.doi.org/10.1016/S0166-2481(06)31017-3.

Plaza A., Benediktsson J.A., Boardman J., Brazile J., Bruzzone L., Camps-Valls G., Chanussot J., Fauvel M., Gamba P., Gualtieri J.A., Marconicini M., Tilton J. C., Trianni G. (2009) - *Recent advances in techniques for hyperspectral image processing*. Remote Sensing of Environment, 113: 110-122. doi: http://dx.doi.org/10.1016/j.rse.2007.07.028.

Porter W.M., Enmark H.T. (1987) - *A system overview of the Airborne Visible/Infrared Imaging Spectrometer (AVIRIS)*. In: Proceedings of the 31st Annual International Technical Symposium, Society of Photo-Optical Instrumentation Engineers (SPIE), 834, pp. 22-31.

Poulet F., Gomez C., Bibring J.P., Langevin Y., Gondet B., Pinet P., Belluci G., Mustard J.

(2007) - *Martian surface mineralogy from Observatoire pour la Minéralogie, l'Eau, les Glaces et l'Activité on board the Mars Express spacecraft (OMEGA/MEx): global mineral maps*. Journal of Geophysical Research, 112: E08S02. doi: http://dx.doi.org/10.1029/2006JE002840.

Selige T., Böhner J., Schmidhalter U. (2006) - *High resolution topsoil mapping using hyperspectral image and field data in multivariate regression modelling procedures*. Geoderma, 136: 235-244. doi: http://dx.doi.org/10.1016/j.geoderma.2006.03.050.

Sumfleth K., Duttmann R. (2007) - *Prediction of soil property distribution in paddy soil landscapes using terrain data and satellite information as indicators*. Ecological Indicators, 8: 485-501. doi: http://dx.doi.org/10.1016/j.ecolind.2007.05.005.

Summers D., Lewis M., Ostendorf B., Chittleborough D. (2011) - *Visible near infrared reflectance spectroscopy as a predictive indicator of soil properties.* Ecological Indicators, 11 (1): 123-131. doi: http://dx.doi.org/10.1016/j.ecolind.2009.05.001.

Ufer K., Kleeberg R., Bergmann J., Curtius H., Dohrmann R. (2008) - *Refining real structure parameters of disordered layer structures within the Rietveld method.* Zeitschrift für Kristallographie Supplements, 27: 151-158. doi: http://dx.doi.org/10.1524/zksu.2008.0020.

Ufer K., Roth G., Kleeberg R., Stanjek H., Dohrmann R., Bergmann J. (2004) - *Description of X-ray powder pattern of turbostratically disordered layer structures with a Rietveld compatible approach*. Zeitschrift für Kristallographie, 219: 519-527. doi: http://dx.doi.org/10.1524/zkri.219.9.519.44039.

van der Meer F. (1995) - *Spectral reflectance of carbonate mineral mixtures and bidirectional reflectance theory: quantitative analysis for application in remote sensing.* Remote Sensing Review, 13: 67-94. doi: http://dx.doi.org/10.1080/02757259509532297.

Vane G., Goetz A.F.H. (1988) - *Terrestrial imaging spectroscopy*. Remote Sensing of Environment, 24: 1-29. doi: http://dx.doi.org/10.1016/0034-4257(88)90003-X.

Viscarra Rossel R.A., McGlynn R.N., McBratney A.B. (2006a) - *Determining the composition of mineral-organic mixes using UV–VIS-NIR diffuse reflectance spectroscopy*. Geoderma, 137: 70-82. doi: http://dx.doi.org/10.1016/j.geoderma.2006.07.004.

Viscarra Rossel R.A., Walvoort D.J.J., McBratney A.B., Janik L.J., Skjemstad J.O. (2006b) - *Visible, near infrared, mid infrared or combined diffused reflectance spectroscopy for simultaneous assessment of various soil properties.* Geoderma, 131: 59-75. doi: http://dx.doi.org/10.1016/j.geoderma.2005.03.007.

Walvoort D.J.J., McBratney A. (2001) - *Diffuse reflectance spectrometry as a proximal sensing tool for precision agriculture*. In: G. Grenier and S. Blackmore (Eds.), Third European Conference on Precision Agriculture, ECPA, vol. 1, Agro Montpellier, Montpellier, France, pp. 503-507.

Received 26/07/2012, accepted 22/09/2012